

Charge-Transfer Forces in the Self-Assembly of Heteromolecular Reactive Solids: Successful Design of Unique (Single-Crystal-to-Single-Crystal) Diels–Alder Cycloadditions

J. H. Kim, S. V. Lindeman, and J. K. Kochi*

Contribution from the Department of Chemistry, University of Houston, Houston, Texas 77204-5641

Received January 11, 2001. Revised Manuscript Received March 9, 2001

Abstract: Electron donor/acceptor (EDA) interactions are found to be a versatile methodology for the engineering of reactive heteromolecular crystals. In this way, a series of the charge-transfer π -complexes between bis(alkylimino)-1,4-dithiin acceptors and anthracene donors are shown to form heteromolecular (1:1) crystalline solids that spontaneously undergo stereoselective [2 + 4] Diels–Alder cycloadditions. The flexible nature of the 1,4-dithiin moiety allows this homogeneous topochemical transformation to proceed with minimal distortion of the crystal lattice. As a result, a unique (single) crystal phase of the Diels–Alder adduct can be produced anti-thermodynamically with a molecular arrangement very different from that in solvent-grown crystals. Such a topochemical reaction between bis(methylimino)-1,4-dithiin and anthracene proceeds thermally and homogeneously up to very high conversions without disintegration of the single crystal. This ideal case of the mono-phase topochemical conversion can be continuously monitored structurally (X-ray crystallography) and kinetically (NMR spectroscopy) throughout the entire range of the crystalline transformation. The resultant “artificial” crystal of the Diels–Alder adduct is surprisingly stable despite its different symmetry and packing mode compared to the naturally grown (thermodynamic) crystal.

Introduction

Solid-state chemical reactions, despite the great potential advantages of enhanced stereo- and regioselectivity,¹ environmental-friendly solvent-free conditions,² and high crystallinity of the products,^{3–5} still remain rather limited in practical applications. Although the vast majority of important (bimolecular) chemical processes are heteromolecular ($A + B \rightarrow C$), most of the solid-state processes are restrictively homomolecular ($2A$

or $2B \rightarrow C$), simply because the cocrystallization of two or more chemically different reagents within the same crystal lattice represents a formidable experimental challenge.⁶ Moreover, the convenient chemical processes in solution are usually thermally promoted, whereas most of the known solid-state reactions are induced photochemically⁸ and have some additional specific (preparative) requirements.⁹

We believe that practically useful solid-state chemical transformations can be significantly expanded by exploiting electron donor/acceptor (EDA) interactions for crystal design.¹⁰ Since many practically important chemical reactions proceed

(1) (a) Hasegawa, M.; Chung, C.-M. *J. Am. Chem. Soc.* **1991**, *113*, 7311, (b) Addadi, L.; Lahav, M. *J. Am. Chem. Soc.* **1979**, *101*, 2152, (c) Mil, J. V.; Addadi, L.; Gati, E.; Lahav, M. *J. Am. Chem. Soc.* **1982**, *104*, 3429, (d) Mil, J. V.; Addadi, L.; Lahav, M. *Tetrahedron* **1987**, *43*, 1281, (e) Tanaka, K.; Toda, F.; Mochizuki, E.; Yasui, N.; Kai, Y.; Miyahara, I.; Hirotsu, K. *Angew. Chem., Int. Ed.* **1999**, *38*, 3523, (f) Foxman, B. M.; Wheeler, K. A. *Chem. Mater.* **1994**, *6*, 1330, (g) Foxman, B. M.; Wheeler, K. A. *Mol. Cryst. Liq. Cryst.* **1992**, *211*, 347, and (h) Coates, G. W.; Dunn, A. R.; Henling, L. M.; Ziller, J. W.; Lobkovsky, E. B.; Grubbs, R. H. *J. Am. Chem. Soc.* **1998**, *120*, 3641. For reviews, see also: (i) Keating, A. E.; Garcia-Garibay, M. A. In *Organic and Inorganic Photochemistry*; Ramamurthy, V.; Schanze, K. S., Eds.; Marcel Dekker: New York, 1998; pp 195–248 and (j) Ramamurthy, V.; Venkatesan, K. *Chem. Rev.* **1987**, *87*, 433.

(2) Tanaka, K.; Toda, F. *Chem. Rev.* **2000**, *100*, 1025.

(3) Crystallinity (in situ) is especially important for polymers (and other slightly soluble compounds) that otherwise are difficult to crystallize by conventional procedures from solution. See: (a) Enkelmann, V. *Adv. Polym. Sci.* **1984**, *63*, 91, (b) Hasegawa, M. *Chem. Rev.* **1983**, *83*, 507, (c) Schwörer, H. E. M.; Huber, R.; Bloor, D. *Chem. Phys. Lett.* **1976**, *42*, 342, and (d) Xiao, J.; Yang, M.; Lauher, J. W.; Fowler, F. W. *Angew. Chem., Int. Ed.* **2000**, *39*, 2132.

(4) Solid-state reactions can be used to prepare single crystals of product (different from those obtained from solution), which may be technically important if they possess some unique physical properties (see: Cohen, M. D. *Tetrahedron* **1987**, *43*, 1211.)

(5) Crystalline matrices can allow the production and stabilization of highly reactive/transient species difficult to isolate from solutions. See: (a) Schlichting, I. *Acc. Chem. Res.* **2000**, *33*, 532 and also (b) Nikishin, G. I.; Koritskii, A. T.; Lindeman, S. V.; Gerr, R. G.; Struchkov, Y. T.; Starostin, E. K. *J. Am. Chem. Soc.* **1989**, *111*, 9214.

(6) Additional specific requirements include size/shape compatibility of the molecular components⁷ and significant strength of the heteromolecular interactions, as compared with the corresponding homomolecular interactions i.e., $E_{A \cdots B} > E_{A \cdots A}$ and $E_{B \cdots B}$. For a detailed analysis of the problem see: (a) Desiraju, G. R.; Sarma, J. A. R. P. *J. Chem. Soc., Chem. Commun.* **1983**, 45, and (b) Desiraju, G. R. *J. Chem. Soc., Chem. Commun.* **1997**, 1475.

(7) Kitaigorodsky, A. I. *Mixed Crystals*; Springer-Verlag: New York, 1984.

(8) The severe restrictions imposed on chemical reactivity by the solid state (the fixed distance and orientation between reaction centers together with the limited motion of molecules in a crystal) result in a higher activation energy needed to initiate the chemical process. This excessive activation energy can be better delivered by photoirradiation (than thermally). For the crystal lattice control of the solid-state reaction, see: (a) Cohen, M. D.; Schmidt, G. M. J.; Sonntag, F. I. *J. Chem. Soc.* **1964**, 2000, (b) Schmidt, G. M. J. *Pure Appl. Chem.* **1971**, *27*, 647, (c) Fu, T. Y.; Liu, Z.; Scheffer, J. R.; Trotter, J. *J. Am. Chem. Soc.* **1993**, *115*, 12202, and (d) Enkelmann, V.; Wegner, G.; Novak, K.; Wagener, K. B. *J. Am. Chem. Soc.* **1993**, *115*, 10390. (e) Zimmerman, H. E.; Zuraw, M. J. *J. Am. Chem. Soc.* **1989**, *111*, 7974.

(9) Strong light absorption in solids in absence of molecular diffusion prevents a uniform delivery of photonic energy over the entire volume of the crystal. However, there have been ingenious attempts to effect solid-state photoreactions under more “homogeneous” conditions. See: (a) Hosomi, H.; Ohba, S.; Tanaka, K.; Toda, F. *J. Am. Chem. Soc.* **2000**, *122*, 1818, and (b) Novak, K.; Enkelmann, V.; Wegner, G.; Wagener, K. B. *Angew. Chem., Int. Ed. Engl.* **1993**, *32*, 1614.

via an EDA complex as a key intermediate,¹¹ crystallization of these intermediates (particularly charge-transfer complexes) followed by consequent topochemical¹² reactions can have important advantages in the following ways:

(a) EDA interactions usually possess enough energy to bring a variety of chemically different components together within the same crystal¹³ and open wide possibilities for carrying out *heteromolecular* solid-state reactions.

(b) Typically, charge-transfer interactions occur *specifically* between chemical partners¹¹ which dramatically increase the probability for these groups to be *juxtaposed* within the crystal for effective chemical interaction.¹⁴

(c) Substantial polarization of the EDA complex can contribute directly in effectively reduced activation energy for the solid-state chemical reaction. A broad-spectrum photoactivation also becomes less problematic because the specific absorption band of the charge-transfer complex can be *selectively* irradiated to initiate a particular chemical transformation.

Nevertheless, the usefulness of EDA complex formation for the crystal engineering of reactive solids has not been fully realized.¹⁵ Recently, we found that EDA complexes can be successfully utilized in a *series* of heteromolecular solids for effecting various [2 + 2] cycloadditions photochemically.¹⁶

In the further pursuit of these objectives, we turned our attention toward reactive EDA solids in which (a) the solid-state reactions are induced thermally,⁹ and (b) the topochemical transformations occur *homogeneously* within the same crystal lattice.¹⁷ This would permit continuous thermodynamic, kinetic, and structural control over the reaction,¹⁸ as well as the spontaneous assembly of product molecules in a crystalline order dictated by that of the starting material and not that limited by

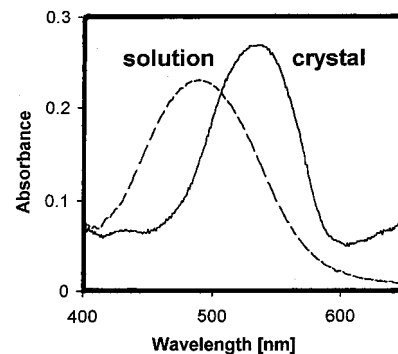


Figure 1. The charge-transfer absorption band of the 1:1 EDA complex of 1,4-dithiin and anthracene in the crystal and in chloroform solution (as indicated).

crystallization techniques. The [2 + 4] cycloaddition of bis(imino)-1,4-dithiins with anthracenes¹⁹ conforms to these requirements because it occurs readily in solution thermally via the 1:1 EDA complex, and the 1,4-dithiin ring system enjoys sufficient conformational flexibility to minimize undesirable intermolecular repulsions during the topochemical process.^{19b,20} We indeed succeeded recently in obtaining a series of reactive crystalline EDA complexes and described a thermal topochemical reaction between bis(ethylimino)-1,4-dithiin and anthracene.²¹ However, this cycloaddition proceeds as a mono-phase up to only 50% conversion, whereupon the crystal lattice of the product unfortunately collapses into the naturally occurring (thermodynamically favored) crystal phase on a time scale comparable with the rate of the continuing solid-state reaction. In addition, an anisotropic (one-dimensional) heterogeneous propagation complicated the single-crystal transformation.

We now report a much improved mono-phase solid-state reaction between bis(methylimino)-1,4-dithiin and anthracene which proceeds homogeneously with a *quantitative* yield²² and results in a new, stable (single) crystal phase of the product which mimics the crystal structure of the starting EDA complex but distinctly differs from the naturally occurring crystals. Importantly, the thermal mono-phase reaction permitted a rare opportunity to make reliable (solid-state) measurements of the thermodynamic parameters and kinetics, as well as to continuously monitor the reaction—not only by X-ray powder diffraction but also by X-ray single-crystal structure analysis—throughout the entire range of crystal conversions.

Results

1. Formation of the Charge-Transfer Complex in the Solid State. A bright red coloration appeared immediately upon the

(18) In heterogeneous (as opposed to homogeneous) topochemical processes, the reaction progresses at the interface between the reactant and the product crystal lattices. Such reactions are substantially controlled by the free-energy changes during the lattices transformations and result in complicated thermodynamic and kinetic evaluations. See: Koga, N.; Tanaka, H. *J. Phys. Chem.* **1994**, *98*, 10521.

(19) (a) Draber, W. *Chem. Ber.* **1967**, *100*, 1559 and (b) Hayakawa, K.; Mibu, N.; Osawa, E.; Kanematsu, K. *J. Am. Chem. Soc.* **1982**, *104*, 7136.

(20) The dihedral angle between two S=C=C-S planes in dithiin derivatives is easily distorted, as seen from the studies of (a) Howell, P. A.; Curtis, R. M.; Lipscomb, W. N. *Acta Crystallogr.* **1954**, *7*, 498 and (b) Dollase, W. A. *J. Am. Chem. Soc.* **1965**, *87*, 979. This flexibility provided reasonable hope that the Diels–Alder adduct formation could be tuned to the crystal environment via the corresponding conformational changes.

(21) Kim, J. H.; Hubig, S. M.; Lindeman, S. V.; Kochi, J. K. *J. Am. Chem. Soc.* **2001**, *123*, 87.

(22) As based on the theoretical yield for random bimolecular reactions in one-dimensional arrays.^{27b} This solid-state yield cannot exceed 86.5% according to combinatorial considerations owing to the remainder of starting molecules left without a reactive partner.

(10) For use of EDA forces in crystal engineering, see: (a) Foster, R. *Organic Charge-Transfer Complexes*; Academic Press: New York, 1969, and (b) Foster, R., Ed. *Organic Molecular Association*; Academic Press: New York, 1975 and 1979; Vols. 1 and 2 and references therein.

(11) (a) Kochi, J. K. *Acc. Chem. Res.* **1992**, *25*, 39. (b) Rathore, R.; Kochi, J. K. *Adv. Phys. Org. Chem.* **2000**, *35*, 193.

(12) According to the classical definition of Kohlschütter, the properties and nature of the products in topochemical reactions are determined by reactions that occur within or on the surface of the solid; see: Kohlschütter, H. W. Z. *Anorg. Allg. Chem.* **1918**, *105*, 121.

(13) See, e.g.: (a) Blackstock, S. C.; Poehling, K.; Greer, M. L. *J. Am. Chem. Soc.* **1995**, *117*, 6617, and (b) McGee, B. J.; Rogers, R. D.; Blackstock, S. C. *Angew. Chem., Int. Ed. Engl.* **1997**, *36*, 1864.

(14) Utilization of alternative intermolecular forces such as hydrogen bonds, Coulombic interactions, etc. (see ref 6b) usually only results indirectly in bringing reaction centers together in crystals. However, an interesting example of more elaborated topochemical alignment of molecules using an H-bonding template was reported recently by MacGillivray, L. R.; Reid, J. L.; Ripmeester, J. A. *J. Am. Chem. Soc.* **2000**, *122*, 7817.

(15) For the relatively few examples of topochemical reactions in the crystals designed by EDA forces, see: (a) Suzuki, T. *Pure Appl. Chem.* **1996**, *68*, 281, (b) Endo, K.; Koike, T.; Sawaki, T.; Hayashida, O.; Masuda, H.; Aoyama, Y. *J. Am. Chem. Soc.* **1997**, *119*, 4117, (c) Suzuki, T.; Fukushima, T.; Yamashita, Y.; Miyashi, T. *J. Am. Chem. Soc.* **1994**, *116*, 2793, (d) Hesse, K.; Hüning, S. *Liebigs Ann. Chem.* **1985**, *715*, (e) Köhler, W.; Novak, K.; Enkelmann, V. *J. Chem. Phys.* **1994**, *101*, 10474 and ref 9b, (f) Coates, G. W.; Dunn, A. R.; Henling, L. M.; Ziller, J. W.; Lobkovsky, E. B.; Grubbs, R. H. *J. Am. Chem. Soc.* **1998**, *120*, 3641.

(16) (a) Bosch, E.; Hubig, S. M.; Lindeman, S. V.; Kochi, J. K. *J. Org. Chem.* **1998**, *63*, 592, (b) Bosch, E.; Hubig, S. M.; Kochi, J. K. *J. Am. Chem. Soc.* **1998**, *120*, 386, and (c) Sun, D.; Hubig, S. M.; Kochi, J. K. *J. Org. Chem.* **1999**, *64*, 2250.

(17) Such transformations are known as “single-crystal-to-single-crystal” reactions. *Homogeneous* crystalline transformations (hereinafter also referred to as “mono-phase” topochemical reactions) are to be distinguished from other (*heterogeneous* or “bi-phase”) single-crystal-to-single-crystal transformations in which a new (product) crystalline phase grows topotactically but separately within the original (reactant) crystal phase. See: (a) Nakanishi, H.; Jones, W.; Thomas, J. M. *J. Phys. Chem.* **1981**, *85*, 3636, (b) Honda, K.; Nakanishi, F.; Feeder, N. *J. Am. Chem. Soc.* **1999**, *121*, 8246, (c) Jordanis, L.; Kanatzidis, M. *Angew. Chem., Int. Ed.* **2000**, *39*, 1928, and (d) Wang, W.-N.; Jones, W. *Tetrahedron* **1987**, *43*, 1273.

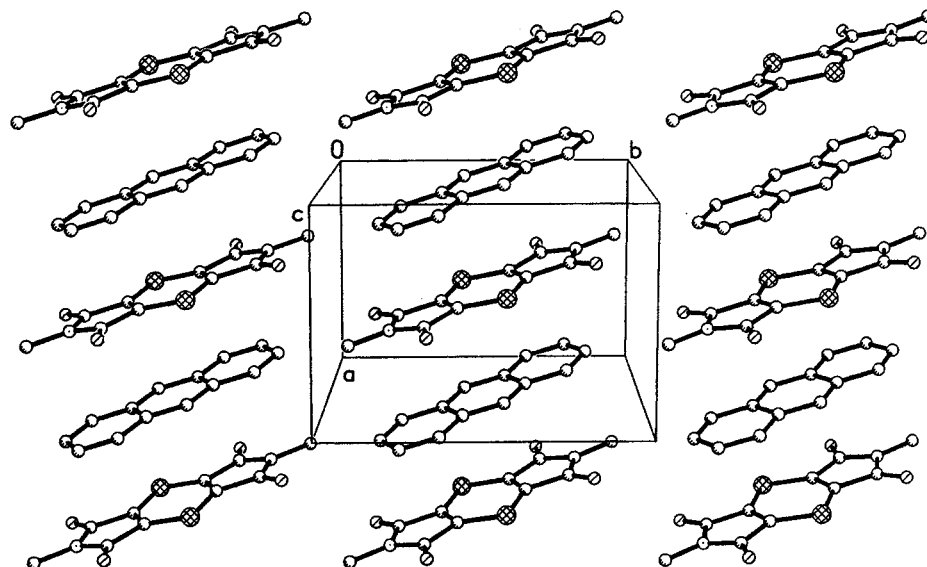
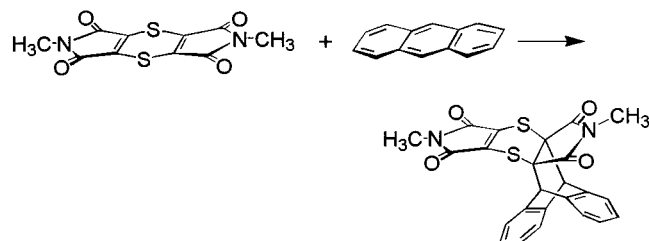


Figure 2. Crystal structure of the 1,4-dithiin/anthracene EDA complex, showing the formation of regular alternate donor/acceptor stacks.

Scheme 1



addition of anthracene to a solution of bis(*N*-methylimino)-1,4-dithiin in dichloromethane. UV/vis spectroscopic analysis of the mixture revealed the appearance of a new (well-resolved) absorption band between 420 and 560 nm ($\lambda_{\text{max}} = 489$ nm) where neither anthracene nor the 1,4-dithiin absorb (Figure 1). This new absorption was assigned to a charge-transfer (CT) transition in the corresponding EDA complex, as established by its adherence to the Mulliken correlation.²³ The molar donor/acceptor ratio of 1:1 for the CT complex in solution was evaluated by the Jobs plot²⁵ (see Supporting Information).

X-ray crystal structure analysis showed that the EDA complex also crystallizes in the same 1:1 ratio, and its structure consists of regular alternate stacks of cofacially oriented anthracene and 1,4-dithiin molecules (Figure 2). The two olefinic bonds of the 1,4-dithiin ring approach the centers of the anthracenes above and below the ring at a distance of $d = 3.38$ Å. It is noteworthy that the charge-transfer band in the solid-state (diffuse reflectance) spectrum of the EDA complex exhibits a significant redshift as compared with that in solution (Figure 1)—possibly owing to delocalization of the electron density along the stacks.

(23) The charge-transfer absorption (λ_{CT}) generally occurs in the UV–vis region with $hc/\lambda_{\text{CT}} = \text{IP} - \text{EA} - \omega$, where IP is the ionization potential of the donor and EA is the electron affinity of the electron acceptor.²⁴ The observed new absorption band undergoes a hypsochromic shift ($\lambda_{\text{max}} = 447$ nm) when anthracene was replaced by its electron-poor 9-bromo analogue, and progressive bathochromic shift when anthracene was replaced by its electron-rich 9-methyl and 9,10-dimethyl analogues ($\lambda_{\text{max}} = 519$ nm for 9-methylanthracene; 566 nm for 9,10-dimethyl anthracene).²¹

(24) (a) Mulliken, R. S. *J. Am. Chem. Soc.* **1952**, *74*, 811. (b) Mulliken, R. S.; Person, W. B. *Molecular Complexes*; Wiley: New York, 1969.

(25) The absorbance at $\lambda_{\text{max}} = 489$ nm was measured for various molar ratios of anthracene and the 1,4-dithiin. The largest (molar) value was obtained for an equimolar mixture to confirm the 1:1 complex formation between anthracene and 1,4-dithiin in dichloromethane solution according to Job, P. *Ann. Chem.* **1928**, *9*, 113.

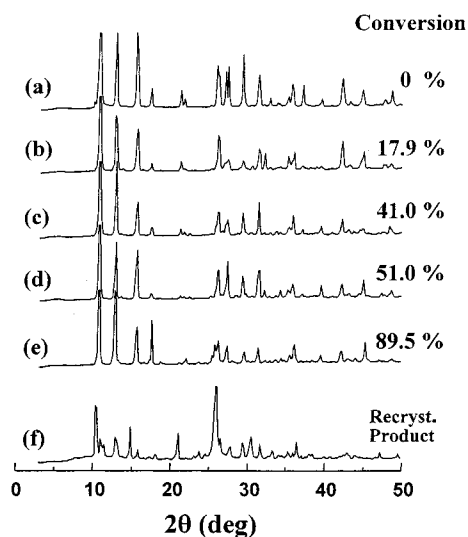


Figure 3. Temporal evolution of the powder diffraction diagram of the 1,4-dithiin/anthracene EDA complex at 50 °C (a–e). For comparison, the powder diffraction pattern of the Diels–Alder cycloadduct crystallized from dichloromethane solution is shown in (f).

Such a close cofacial orientation of the donor and acceptor moieties represents an ideal arrangement for the solid-state Diels–Alder [2 + 4] cycloaddition reaction in the crystal.

2. Single-Crystal-to-Single-Crystal Transformation during Diels–Alder Cycloaddition. The heteromolecular CT crystals of the 1,4-dithiin acceptor and anthracene donor slowly reacted at room temperature to yield a single product of the [2 + 4] Diels–Alder cycloaddition (Scheme 1).

Concomitantly, the bright red color of the CT crystals uniformly bleached to pale yellow. The thermal solid-state reaction also carried out at several higher temperatures (50, 60, 70, and 80 °C) consistently afforded the same product. The powder X-ray diffraction study revealed *no formation of any new crystalline or amorphous phase* during the reaction (Figure 3). The X-ray diffraction patterns exhibited only limited changes in the position/intensity of the peaks to indicate merely small (continuous) lattice distortions accompanied by relatively minor structural changes. Note that the diffraction pattern of the product of the topochemical conversion differs dramatically from

Table 1. Crystallographic Parameters and Refinement Data for CT Crystals at Different Degrees of Topochemical Conversion

conversion (%)	0	29.7	35.2	80.0	85.9	100 ^a
<i>a</i> (Å)	7.150(1)	7.174(1)	7.186(1)	7.293(1)	7.313(1)	8.632(1)
<i>b</i> (Å)	10.216(2)	10.202(1)	10.207(1)	10.110(1)	10.120(1)	10.202(1)
<i>c</i> (Å)	13.723(2)	13.765(1)	13.784(2)	13.824(1)	13.859(2)	11.555(1)
α (deg)	90	90	90	90	90	76.965(1)
β (deg)	91.438(4)	92.135(1)	92.279(2)	94.179(1)	94.389(3)	87.413(1)
γ (deg)	90	90	90	90	90	69.558(1)
<i>V</i> (Å ³)	1002.1(5)	1006.7(2)	1010.2(3)	1016.6(1)	1022.6(4)	991.9(1)
<i>d</i> (g cm ⁻³)	1.526	1.519	1.514	1.504	1.496	1.542
R1	0.045	0.058	0.063	0.072	0.067	0.029
<i>N</i> [<i>I</i> > 2 σ (<i>I</i>)]	3389	3236	3654	3131	3330	7371

^a Data for the recrystallized [4 + 2] Diels–Alder product, for comparison.

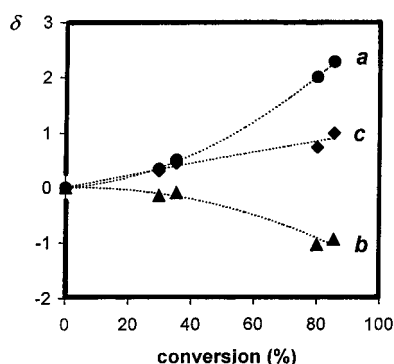


Figure 4. Relative changes in cell parameters *a*, *b*, and *c* (%) of the 1,4-dithiin/anthracene complex at different degrees of conversion of the topochemical reaction in Scheme 1.

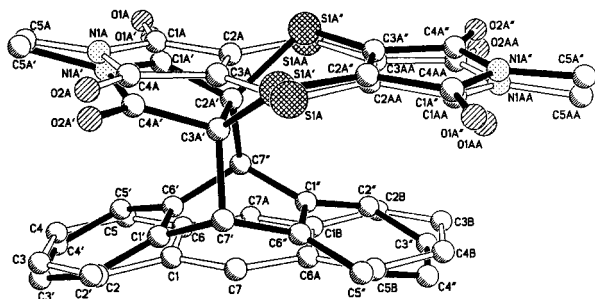


Figure 5. Changes in the atomic positions of the 1,4-dithiin and anthracene EDA complex (white bonds) relative to the Diels–Alder [2 + 4] cycloaddition product (black bonds) obtained from the topochemical conversion.

the X-ray diffraction pattern of the recrystallized product (Figure 3f).

Importantly, the solid-state reaction did not diminish the quality of the single crystals of the complex even at very high (chemical) conversions.²⁶ Thus, the single-crystal X-ray structure analyses were carried out at various degrees of conversion to monitor the changes in the crystal lattice parameters and atomic movements in the reactant lattice during formation of the Diels–Alder cycloadduct. Table 1 shows the evolution of the unit cell dimensions of the CT crystals with the degree of the topochemical conversion. The relative changes of the cell parameters on going from the reactant to the product are represented in Figure 4. As one can see, the cell parameters *a* and *c* gradually increased (within 2.5%), whereas *b* decreased (within 1.0%) during the completion of the crystal conversion. Figure 5 illustrates the structural changes between the reactant and

(26) The single crystals remained optically transparent and changed color uniformly. Mechanical cracking was apparent only for relatively large crystals. The diffraction intensity diminished slightly at high-angle reflections, as expected for a disordered crystal structure.

Table 2. Changes in Atomic Positions *d* (Å) during the Solid-State Topochemical Reaction^a

vector	<i>d</i>	vector	<i>d</i>	vector	<i>d</i>
C1 → C1'	0.48	S1A → S1A'	0.30	C2AA ^c → C2A''	0.18
C2 → C2'	0.11	O1A → O1A'	0.49	C3AA ^c → C3A''	0.24
C3 → C3'	0.31	O2A → O2A'	0.61	C4AA ^c → C4A''	0.32
C4 → C4'	0.25	N1A → N1A'	0.49	C5AA ^c → C5A''	0.35
C5 → C5'	0.19	C1A → C1A'	0.53		
C6 → C6'	0.48	C2A → C2A'	0.99		
C7 → C7'	0.97	C3A → C3A'	1.03		
C1B ^b → C1''	0.58	C4A → C4A'	0.65		
C2B ^b → C2''	0.21	C5A → C5A'	0.29		
C3B ^b → C3''	0.50	S1AA ^c → S1A''	0.24		
C4B ^b → C4''	0.52	O1AA ^c → O1A''	0.31		
C5B ^b → C5''	0.26	O2AA ^c → O2A''	0.41		
C6A ^b → C6''	0.52	N1AA ^c → N1A''	0.31		
C7A ^b → C7''	1.19	C1AA ^c → C1A''	0.21		

^a The data are for a crystal with 80% conversion. See Figure 5. ^b Atoms C1B through C7A are symmetry equivalents of the atoms C1 through C7, respectively. ^c Atoms S1AA through C5AA are symmetry equivalents of the atoms S1A through C5A, respectively.

cycloaddition product, while a detailed list of the atomic movements during the solid-state reaction is given in Table 2. Most importantly, the product molecules are reproducibly oriented within the reactant crystal lattice without a noticeable change in the crystallographic positions of the reactant molecules.

The molecular and crystal structure of the topochemical product was compared with that of the recrystallized product. All of the molecular geometrical parameters are virtually identical in the two different crystal modifications (see Supporting Crystallographic Information). It is particularly interesting to note that the folding of the 1,4-dithiin moiety is quite similar in the topochemical product (136.7°) and in the recrystallized product (132.2°).

The packing modes in the two crystal modifications of the Diels–Alder adduct are remarkably different (see Figure 6). Whereas the packing of the solid-state cycloaddition product closely mimics the structure of the original CT crystal, with an alternate arrangement of anthracene and 1,4-dithiin moieties along the crystal stack (Figure 6a), the packing of the recrystallized product showed a “dimeric” molecular association of both dithiin and anthracene moieties, separately (Figure 6b). In other words, the topochemical product exhibits a continuous “head-to-tail” molecular arrangement, but the recrystallized product is arranged pairwise in a “head-to-head”/“tail-to-tail” sequence.

3. Kinetic Observations on the Solid-State Diels–Alder Reaction. The solid-state reaction in the crystalline powder was carried out at different temperatures (viz. 50, 60, 70, and 80 °C), and the rate of conversion was monitored by ¹H NMR spectroscopy (see Experimental Section). The progress with time is shown in Figure 7a at various temperatures. Most notably, the rate of the reaction increased substantially with the

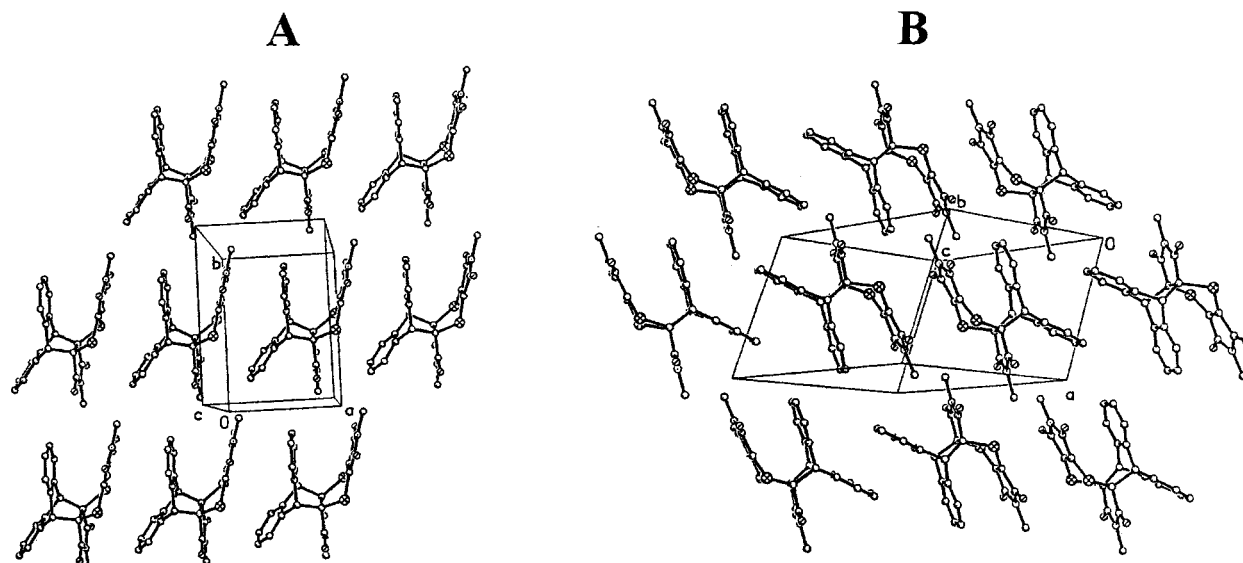


Figure 6. Idealized crystal structure of the topochemical [2 + 4] cycloaddition product (A) as compared with the crystal structure of the product naturally grown from dichloromethane solution (B).

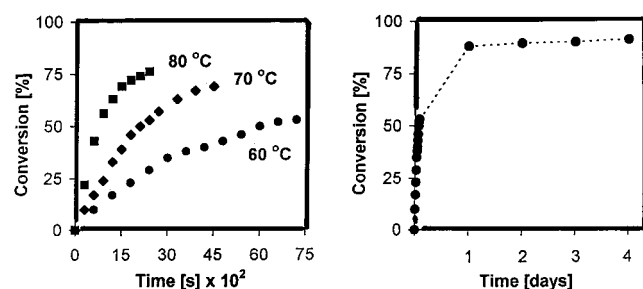


Figure 7. Conversion/time profiles of the solid-state reaction between the 1,4-dithiin and anthracene monitored at different temperatures (A), and in a long run of 4 days at 60 °C (B).

temperature—the half-life of the starting material being 140 min at 60 °C, 35 min at 70 °C, and only 12 min at 80 °C. The conversion increased linearly with time only at the beginning of the reaction; then the rate of conversion gradually slowed and ultimately came to saturation (i.e., did not exhibit any further noticeable changes) after 4 days at 60 °C (see Figure 7b). The kinetic behavior of the thermal solid-state bimolecular (donor/acceptor) reaction was taken to be first-order at low conversions (see eq 1, Scheme 2).

However, in the so-called β -crystals, each reactant molecule initially has two equivalent partners with which to react—but these are gradually replaced by one-sided and isolated molecules (i.e., surrounded by the nonreactive product from one or both sides, respectively) which continually accumulate during the course of reaction. As a result, the effective rate of the reaction slows down as compared to the simple first-order process, and the final chemical conversion never attains 100%.

A kinetic model for the β -crystals has been proposed on the basis of a statistical analysis (see eq 2, Scheme 2).²⁷ The distribution of all the reactant molecules having different environments in the crystal (two-sided reactant, one-sided reactant, and isolated molecules) is taken into consideration in this approach, and the solution of the corresponding differential equation has the biexponential form presented in eq 3, Scheme 2. Thus, the plots of $\ln(C/C_0)$ versus time have been utilized to

Scheme 2

$$\frac{dc}{dt} = -k_1c \quad (1)$$

$$\frac{dc}{dt} = -k_1(c_2 + c_1/2) \quad (2)$$

where c_2 is the concentration of the molecules having 2 partners to react:

$$c_2 = P(1-P_d)^2 + 2P(1-P_d) + (1-3P)(1-P_d)^2 \\ = (1-2P)c^2/(1-P)^2 - 2c + 1$$

and c_1 is the concentration of the molecules having 1 partner to react:

$$c_1 = -c^2/(1-P) + c$$

$$P = 1/e^2 \approx 13.53\% \quad \text{— the average probability of the fraction of the molecules with no partner to react at the condition of reaction.}$$

$$P_d = c/(1-P) \quad \text{— the average probability of the product formation}$$

$$c = (1-P)(e^{k_1t} - 1) / [e^{k_1t} - (1-3P)/2] \quad (3)$$

obtain the rate constants at various temperatures. The calculated curves corresponding to the kinetics of the β -type crystals are superimposed on the experimental data in Figure 8 and compared with the usual first-order approximations (dashed lines). One can see that, whereas the experimental data already start to deviate from first-order kinetics after only 30% conversion, the β -type kinetic model fits the experimental results well throughout almost the entire range. The measured rate constants are presented in Table 3, which also includes the activation energy (E_A) for the solid-state reaction determined from the Arrhenius plots of the rate constants versus the reciprocal temperature.

The preequilibrium constant (K_{EDA}) and the first-order rate constant (k_1) in chloroform solution were also calculated according to Scheme 3.

It is noteworthy that the activation energy E_A for the solid-state cycloaddition was about 2 times larger than that observed in solution. Furthermore, the rate of the solid-state reaction was nearly 6 times slower than that in solution at 50 °C.

(27) (a) Cohen, E. R.; Reiss, H. *J. Chem. Phys.* **1963**, *38*, 680. (b) Wernick, D. L.; Schochet, S. *J. Phys. Chem.* **1988**, *92*, 6773. (c) Harris, K. D. M.; Thomas, J. M. *J. Chem. Soc., Faraday Trans.* **1991**, *87*, 325, and (d) Savion, Z.; Wernick, D. L. *J. Org. Chem.* **1993**, *58*, 2424.

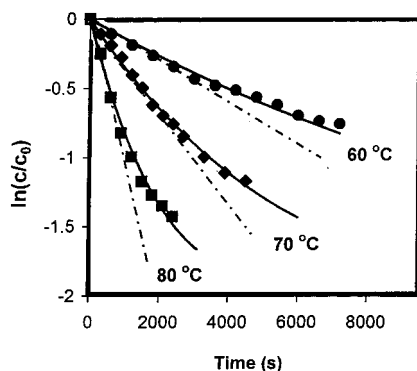


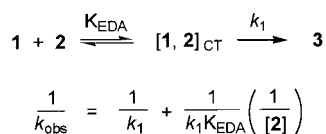
Figure 8. Kinetic evaluation of the solid-state cycloaddition at different temperatures treated as a usual first-order reaction (dashed lines) and as a statistical bimolecular transformation in one-dimensional crystalline arrays (solid lines) according to Scheme 2.

Table 3. Solid-State First-Order Rate Constants k_1 (s^{-1}) at Different Temperatures^a

temp	$k_1 \times 10^{-4}$ (solid state)	$k_1 \times 10^{-4}$ (solution)
80 °C	8.5	-
70 °C	3.2	-
60 °C	1.2	-
50 °C	0.5	3.08
E_A	22.85	12.2

^a The activation energy E_A is given in (kcal/mol).

Scheme 3



Discussion

Charge-Transfer Crystals. Bis(*N*-methylimino)-1,4-dithiin and anthracene form the 1:1 EDA charge-transfer complex in solution which further reacts thermally to yield the Diels–Alder cycloadduct as described in Scheme 1. The complex can be readily isolated in crystalline form by the very slow removal of solvent at low temperatures (to obviate competition from the thermal reaction). In the resulting charge-transfer crystals, the planar molecules of the donor (anthracene) and the acceptor (the 1,4-dithiin) form regular alternate stacks with a small dihedral angle between the mean planes of the cofacial molecules (2.0°) and with close contacts of $d = 3.38 \text{ \AA}$ between the centers of the reacting groups (the ethylene bonds of a pair of 1,4-dithiins lying directly above and below the central ring of anthracene). This cofacial orientation at the close distance represents an ideal arrangement for the solid-state Diels–Alder cycloaddition in the charge-transfer crystals, which is already significant at ambient conditions and accelerates at higher temperatures.

Solution versus Solid-State Diels–Alder Cycloadditions. Steric, electronic, and statistical conditions for the Diels–Alder reaction are obviously not the same in solution and in the crystals. Thus, the reaction in solution proceeds within solvated donor/acceptor couples, has a diffusion-controlled step and obeys pseudo-first-order kinetics (see Scheme 3). On the other hand, the topochemical reaction in the crystal (a) has a modified electronic state of the reactants, as can be seen indirectly from the red-shifted electronic CT spectrum of the donor/acceptor pair compared with that in solution (Figure 1) owing to the formation of continuous regular alternate donor/acceptor stacks (see Figure 2) and not isolated couples. In addition, (b) the

crystal lattice of the reactant imposes some steric and electronic restriction on product formation—the molecule of the product having a (different) shape generally incompatible with the surrounding crystal net, and the product formation inevitably involves breaking the chain of π -conjugation within the stacks. And finally, (c) the reaction in the crystal (in absence of diffusion) has limitations on the availability of partner molecules to interact with (there being molecules with two equivalent partners, with one partner and without a partner) that cause significant deviations from the first-order kinetics during the progress of the reaction (see Scheme 2) and result in an upper statistical limit for the yield of cycloadduct. It is difficult to quantitatively evaluate the particular contributions of the aforementioned factors in the course of the topochemical reaction, but in total they result in an activation energy E_A of the solid-state transformation (22.9 kcal/mol), which is twice as large as that obtained in chloroform solution (12.2 kcal/mol), and in a rate constant $k_1 = 0.5 \times 10^{-4} \text{ s}^{-1}$ which is 6 times smaller than that in solution ($3.1 \times 10^{-4} \text{ s}^{-1}$).

Statistical Limitations on Single-Crystal-to-Single-Crystal Transformations.

A schematic overview of the series of solid-state transformations of the anthracene/dithiin pair in the regular donor–acceptor stacks is given in Figure 9. We can see that at very beginning, each anthracene donor (blue) has two exactly equivalent dithiin acceptors (red) to interact with (according to the crystallographic symmetry, molecules of both donor and acceptor occupy crystallographic centers of symmetry) and reacts randomly in either direction. With the progress of the reaction, there is a growing concentration of donors and acceptors surrounded on one side by the already formed cycloadduct product (black). Generally, the reactivity of these molecules should be different from “two-sided” molecules, but more importantly, they enjoy only half the probability for interaction (and this is reflected by eq 2 in Scheme 2). Finally, at the terminal stages of reaction, there is an accumulation of molecules surrounded on both sides by the already reacted (cycloadduct) product and consequently have no opportunity to react at all.

Our kinetic measurements confirm this mechanistic scheme, as can be seen in Figure 8 which shows good agreement between the experimental points and the calculated curve on the basis of the corresponding mathematical description (Scheme 2).²⁷ Also, the measured yield of the cycloadduct accords well with this representation—the crystallographically measured composition of the completely reacted single crystals giving an almost ideal yield of 85.9%, whereas ¹H NMR measurements on the reacted powder afforded a similar yield (92.6%) at the saturation point of the reaction. In both cases, at saturation the yield is close to the theoretical limit of 86.5%. [It is possible that in the fine powder an additional possibility exists for the surface molecules to diffuse and react at the interface between crystal domains due to the relatively large active surface of the ground material.]

Free Space/Molecular Motion in the Crystal Lattice. In large degree, the relatively smooth course of the topochemical reaction takes place due to our deliberate choice of the 1,4-dithiin “hinge” as a conformationally flexible moiety to reduce the otherwise inevitable steric repulsion between reactant molecules and the formed product. Figure 5 and Table 2 show that one-half of the acceptor molecule actually remains in its place as a result of bending along the $S \cdots S$ axis and the corresponding dihedral angle decreases from 180° in the unreacted acceptor to 136.7° in the reacted cycloadduct (in the recrystallized adduct this angle is almost the same— 132.2°).

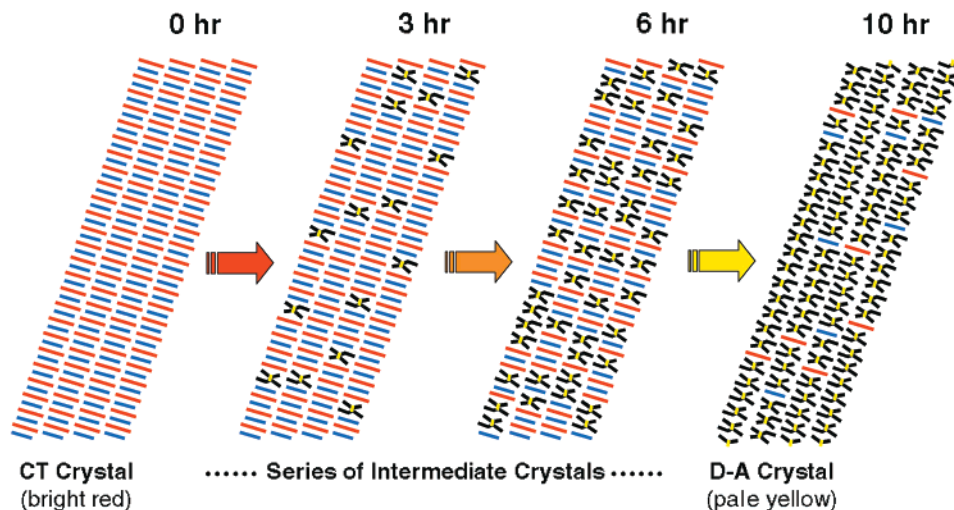


Figure 9. Schematic representation of the progressive (thermal) conversion of the single crystal of CT-complex of the dithiin acceptor and anthracene donor to the single crystal of the [2 + 4] Diels–Alder cycloadduct.

Furthermore, there are only minor changes in the interactions between the stacks of molecules during product formation that would otherwise cause significant (lattice) complications.

It is instructive to compare the course of the topochemical reaction of bis (*N*-methylimino)-1,4-dithiin with that of its closest homologue—bis (*N*-diethylimino)-1,4-dithiin reported earlier.²¹ Although the general mechanistic features of both topochemical reactions are alike, the ethyl homologue during its reaction (with anthracene) suffers a rotation of one of its terminal methyls by 180°. That structure also contains C–H···O hydrogen bonds between the donor/acceptor stacks (otherwise built the same way as the methyl homologue) which are broken during the reaction. As a result, the topochemical reaction of the ethyl homologue has a somewhat increased activation barrier ($E_A = 24.9$ versus 22.9 kcal/mol), whereas in solution the E_A of 12.2 kcal/mol is the same for both acceptors. Moreover, the rate of the ethyl analogue does not slow with solid-state conversion, but even *accelerates* with time. A further difference is shown by the 100% (chemical) conversion attained by the ethyl analogue in the solid state, possibly owing to a limited one- or two-dimensional propagation.

Topochemical Growth of “Artificial” Crystals of the Diels–Alder Adduct. The most important result of the careful design of the solid-state reaction between bis (*N*-methylimino)-1,4-dithiin and anthracene is the topochemical growth of a new crystal modification of the product which has a principally different structure from the conventionally obtained (solvent-grown) crystals. We earlier sought this effect with the anthracene complex of the ethyl homologue,²¹ but the single crystals collapsed into microcrystalline material after only ~50% chemical conversion, and the resultant new (metastable) phase was converted relatively rapidly into the thermodynamically stable phase. With the methyl homologue, the relatively mild topochemical conditions of the reaction (due to minimal conformational rearrangements and the absence of principal changes in intermolecular forces between stacks) enable us to achieve the homogeneous completion of the topochemical reaction without breaking the crystal lattice and formation of any extraneous crystal (or amorphous) phase (see Figure 3). The formation of the product phase proceeds with only minimal distortions in the cell dimensions—only 2.3% expansion of the parameter a along the stacks (for the ethyl homologue the expansion of the corresponding parameter by 2.5% was already observed at 50% conversion), a 1.0% contraction of the

parameter b across the stacks in direction of long axes of the molecules (a similar contraction was observed for the ethyl homologue due to the folding of the 1,4-dithiin and anthracene moieties), and a 1.0% expansion of the parameter c .²⁸ The total density of the crystals becomes 2% lower during the cycloaddition (1.526 g cm⁻³ for the starting donor/acceptor complex and 1.496 g cm⁻³ for the final cycloadduct product), and it significantly turns out to be 3% less than the density of the thermodynamically favored (naturally occurring) phase of 1.542 g cm⁻³.

The new “artificial” modification of the product (although obtained as a centrosymmetric twin with inclusion of 14% of nonreacted starting material) is stable for months to retain its (single) crystallinity. It has a molecular arrangement quite different from that in the naturally occurring crystals. Thus, the artificial modification remains monoclinic to strikingly mimic the crystal order and symmetry of the starting CT complex. (In contrast, the recrystallized product is triclinic). Accordingly, the molecules in the artificial crystals²⁹ are packed in a “tail-to-head” sequence whereas in the natural crystals they exhibit a pairwise “tail-to-tail” and “head-to-head” packing (see schematic representation in Figure 10). We thus consider this to be an important prototypical achievement toward the construction of artificial noncentrosymmetric crystal phases for nonlinear optical and related applications.³⁰

Charge-Transfer Forces in Donor–Acceptor Crystals. The preequilibrium complexation (Scheme 3) of the anthracene donor (D) and the 1,4-dithiin acceptor (A) in chloroform is characterized by a formation constant $K_{EDA} = 2.22 \text{ M}^{-1}$, as determined by the Benesi–Hildebrand spectrophotometric analysis of the charge-transfer absorption band at $\lambda_{\text{max}} = 489 \text{ nm}$ (Figure 1).^{19b} The limited magnitude of K_{EDA} indicates that the intermolecular (charge-transfer) interaction between this D/A

(28) Actually, the cell dimensions were observed to change slower than the progress of the reaction, and it required some time for them to relax to equilibrium values (at a given degree of conversion). Because of this slow change, the actual equilibrium values of the cell dimensions for crystals with incomplete conversion may differ slightly from those given in Table 1.

(29) To be precise, the head-to-tail sequence occurs in continuous domains of the twinned phase (between two nonreacted molecules); after that the sequence switches its direction in the opposite direction (see Figures 9 and 10).

(30) As suggested by a reviewer, the “artificial crystals” in the extreme case (i.e., quantitative yield) represent a polymorph of the “naturally occurring crystals”.

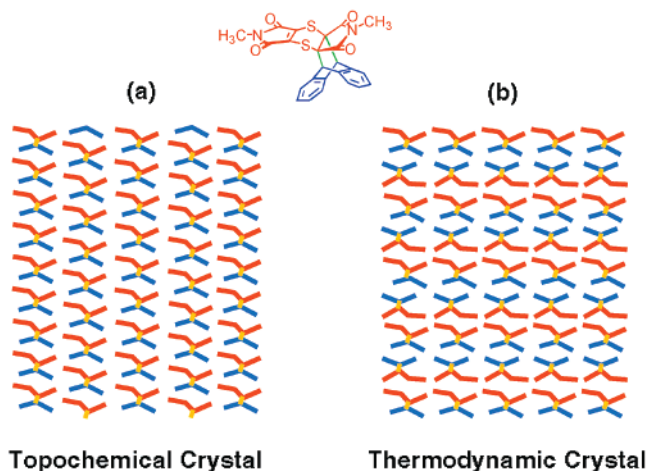


Figure 10. Schematic representation of the different molecular arrangements of the [2 + 4] cycloaddition product in crystals (a) grown topochemically and (b) obtained (thermodynamically) by crystallization from dichloromethane solution.

pair is rather small ($\Delta G \cong 0.5 \text{ kcal mol}^{-1}$) in solution. However, such charge-transfer forces are sufficient in the crystalline state to enforce the cofacial orientation of anthracene and the dithiin donor/acceptor pairs at a close interplanar distance of $d = 3.38 \text{ \AA}$ (see Figure 2), which is less than their van der Waals separation.³¹

The role of charge-transfer forces goes beyond the simple maintaining of the highly ordered steric conditions for the heteromolecular solid-state reaction. According to Mulliken,²⁴ the ground-state of the EDA complex is approximated by:

$$\Psi_{D,A} \cong a\psi_{D,A} + b\psi_{D^+A^-} + \dots \quad (4)$$

where $\psi_{D,A}$ corresponds to the no-bond (van der Waals) association of anthracene and the dithiin, and $\psi_{D^+A^-}$ represents the dative or charge-transfer contribution. Thus, polarization of the ground-state corresponds to the partial (resonance) contribution from the oxidized donor (D^+) and reduced acceptor (A^-), and it is evaluated as the degree of charge-transfer, that is, $b^2/(a + b)^2$.³⁶ As such, the degree of charge transfer increases with donor strength, and leads to increased rates of the ensuing (thermal) Diels–Alder cycloaddition.³⁷ [For example, the activation energy for anthracene of $12.2 \text{ kcal mol}^{-1}$ is lowered to $9.4 \text{ kcal mol}^{-1}$ in the stronger donor 9,10-dimethylanthracene; and the same trend is observed in the preequilibrium constant $K_{EDA} = 2.2 \text{ M}^{-1}$ for anthracene and 20.8 M^{-1} for dimethylanthracene.]^{19b} Since the charge-transfer contribution can be quantitatively evaluated via structural changes,³⁸ we carefully compare

(31) Almost identical packing patterns are found in the EDA complexes of anthracene with bis(*N*-ethylamino)-1,4-dithiin,²¹ *N,N'*-dimethylpyromellitic diimide,³² pyromellitic dianhydride,³³ pyromellitic dithioanhydride,³⁴ and also for acridine complex with the bis(*N*-methylimino)-1,4-dithiin.³⁵

(32) Bulgakovskaya, I. V.; Smelyanskaya, E. M.; Fedorov, Y. G.; Zvonkova, Z. V. *Kristallografiya* **1977**, *22*, 184.

(33) (a) Boeyens, J. C. A.; Herbstein, F. M. *J. Phys. Chem.* **1965**, *69*, 2160 and (b) Robertson, B. E.; Stezowski, J. J. *Acta Crystallogr., Sect. B* **1978**, *34*, 3005.

(34) Bulgakovskaya, I. V.; Smelyanskaya, E. M.; Fedorov, Y. G.; Zvonkova, Z. V. *Kristallografiya* **1974**, *19*, 260.

(35) Yamaguchi, Y.; Ueda, I. *Acta Crystallogr., Sect. C* **1984**, *40*, 113.

(36) (a) Ketelaar, J. A. A. *J. Phys. Radium*. **1954**, *15*, 197. (b) Tamres, M.; Brandon, M. *J. Am. Chem. Soc.* **1960**, *82*, 2134. (c) Hubig, S. M.; Kochi, J. K. *J. Am. Chem. Soc.* **1999**, *121*, 617.

(37) See: Fukuzumi, S.; Kochi, J. K. *Tetrahedron* **1982**, *38*, 1035.

(38) (a) Hubig, S. M.; Lindeman, S. V.; Kochi, J. K. *Coord. Chem. Rev.* **2000**, *200–202*, 831. See also: (b) Le Maguères, P.; Lindeman, S. V.; Kochi, J. K. *Organometallics* **2001**, *20*, 115 and *J. Chem. Soc., Perkin Trans. 2* **2001**. In press.

the geometrical parameters extant in the crystalline anthracene/dithiin complex with those previously measured individually for anthracene³⁹ and bis(*N*-methylimino)-1,4-dithiin.⁴⁰ The observed bond length changes do not exceed 0.5 pm (see Supporting Information) and lie within the experimental errors of even the better (available) data ($3\sigma > 0.6 \text{ pm}$). Accordingly, we can at this juncture only conclude that the degree of charge transfer in the anthracene/dithiin complex is $< 10\%$, as can also be expected from the limited value of K_{EDA} in solution (vide supra).^{38b}

Conclusions

The deliberate use of charge-transfer forces allows the synthesis of heteromolecular crystals that are prearranged for solid-state reaction. Using the derivatives of bis(*N*-alkylimino)-1,4-dithiin and anthracene, we design a series of reactive charge-transfer crystals prone to thermal [2 + 4] Diels–Alder cycloaddition. The judicious choice of the 1,4-dithiin moiety as a flexible joint allows the reaction to proceed with only minor distortions of the crystal lattice up to very high degrees of topochemical conversion. For the 1:1 mixed crystal of bis(*N*-methylimino)-1,4-dithiin and anthracene, an exceptionally smooth course of the thermal topochemical reaction is achieved—with the (single) crystallinity preserved to the theoretical limit of the conversion. Both the kinetics of the reaction and the composition of the product confirm an almost ideal homogenic mono-phase character of the transformation, as continuously monitored by single-crystal X-ray structural analysis. Importantly, the topochemical reaction results in the formation of a new, relatively stable artificial crystal phase with molecular arrangement quite different from that in the naturally crystallized product. This study emphasizes the caveat that effective crystal engineering of heteromolecular stacks of donor/acceptor pairs requires careful attention to subtle changes in component structures (even as minor as the trivial replacement of an ethyl²¹ for a methyl group) that can otherwise disrupt a perfect single-crystal-to-single-crystal transformation!

Experimental Section

Materials and Methods. Benzene and dichloromethane (reagent grade) were stirred over concentrated H_2SO_4 and successively washed with aqueous bicarbonate and water. Benzene was distilled serially from P_2O_5 and from sodium under an argon atmosphere. Dichloromethane was distilled from P_2O_5 and CaH_2 . Chloroform (reagent grade) was stirred over several small portions of concentrated H_2SO_4 , washed with water, and distilled from P_2O_5 under an argon atmosphere. Bis(*N*-methylimino)-1,4-dithiin was prepared and purified by the method of Osawa et al.¹⁹ Anthracene was obtained from Aldrich and used as received. ^1H NMR spectra were recorded in CDCl_3 or $\text{DMSO}-d_6$ with a General Electric QE-300 NMR spectrometer, and the chemical shifts are reported as ppm downfield from an internal tetramethylsilane standard. UV/vis absorption spectra were recorded with a Hewlett-Packard 8453 diode-array spectrometer.

Crystallization of the 1:1 Complex of Anthracene and Bis(*N*-methylimino)-1,4-Dithiin. The 1:1 complex of anthracene and bis(*N*-methylimino)-1,4-dithiin was isolated in crystalline form as bright red needles by the very slow removal of the solvent from an equimolar mixture of anthracene and the 1,4-dithiin in tetrahydrofuran solution (50 mM) at $-4 \text{ }^\circ\text{C}$ over the course of a week.

Crystallization of the Diels–Alder Adduct. The cycloadduct obtained from the solution-phase reaction was dissolved in dichloro-

(39) (a) Ponomarev, V. I.; Shilov, G. V. *Kristallografiya* **1983**, *28*, 674 and (b) Brock, C. P.; Dunitz, J. D. *Acta Crystallogr., Sect. B* **1990**, *46*, 795.

(40) Brisse, F.; Alfani, M.; Bergeron, J.-Y.; Belanger-Gariepy, F.; Armand, M. *Acta Crystallogr., Sect. C* **2000**, *56*, 190.

methane and the solvent was then removed slowly (one week) to produce pale yellow single crystals suitable for X-ray crystallography.

Diffuse-Reflectance Spectroscopy of the Charge-Transfer Crystals. The freshly prepared bright red crystals of the 1:1 complex of anthracene and the 1,4-dithiin were ground into a fine powder and then diluted (5 wt %) with a fine colorless powder of KPF₆. The diffuse-reflectance UV/vis spectrum (Figure 1) was recorded with a Varian Cary 5G spectrometer equipped with an integrating sphere.

X-ray Single-Crystal Structure Analyses. The intensity data were collected at $-150\text{ }^{\circ}\text{C}$ with a Siemens/Bruker SMART diffractometer equipped with an 1K CCD detector using Mo K α -radiation ($\lambda = 0.71073\text{ \AA}$). The structures of the starting EDA complex and recrystallized product were solved by direct methods⁴¹ and conveniently refined by a full matrix least-squares procedure⁴² with IBM Pentium and SGI O₂ computers. For the partially reacted crystals of the complex, the atomic coordinates of the reactant molecules were taken from the native (unreacted) complex structure, and the atomic positions of the product were found in a series of difference Fourier syntheses as a contaminant superposition of two (centrosymmetrically) superimposed components. Positions of some atoms superimposed at distances beyond experimental resolution were added geometrically. The composite structures were refined with reasonable geometrical restrictions using appropriate options of the SHELXL program package:⁴² (i) Total populations of the structures of the complex and the product were kept equal to unity; populations of the two disordered components of the product were kept equal to each other. (ii) Planarity constraints were applied for benzenoid and five-membered imino rings of the product molecule; their geometry was constrained to be the same as that of the parent moieties of the reactants. (iii) Thermal atomic coefficients of closely superimposed atoms of the molecule of the product were restrained to be the same as in the parent reactant molecules. (iv) A riding and rotating model was applied to position all hydrogen atoms with $U_{\text{iso}} = 1.2U_{\text{iso/eq}}$ of an adjacent carbon atom ($1.5U_{\text{iso/eq}}$ for the methyl hydrogens). The pertinent crystallographic data are on deposit at the Cambridge Crystallographic Data Center, U.K.

X-ray Powder Diffraction Study. Samples for the X-ray-powder diffraction were taken as small aliquots from the same freshly crystallized batch of the complex that was heated incrementally at $50\text{ }^{\circ}\text{C}$. Between the heating cycles and measurements, the mother batch was stored at room temperature. The powder diffraction patterns of

the samples were recorded at room temperature with a Phillips 1840 diffractometer using Cu K α radiation ($\lambda = 1.54178\text{ \AA}$) in 0.02° steps over the range: $3^{\circ} < 2\theta < 50^{\circ}$. The degree of conversion at each stage was determined by ¹H NMR spectroscopy after dissolution of the sample in DMSO-*d*₆. The X-ray powder diffraction pattern of the recrystallized product (in dichloromethane solution) was also measured under identical conditions as a standard for comparison.

Kinetics Measurements of the Solid-State Reaction. Crystals of the 1,4-dithiin/anthracene complex were ground and placed (in 10 mg portions) into 20 NMR tubes. The NMR tubes were kept in a thermostated water bath at the specified temperature that is, 50, 60, 70, and 80 $^{\circ}\text{C}$. Periodically, a tube was removed from the bath and its solid content dissolved in DMSO-*d*₆ to record the NMR spectrum. The conversion at a given temperature and time was then calculated from the decrease of the ¹H NMR resonances of the 9- and 10-protons of anthracene.

Kinetics Measurement of the Solution-Phase Reaction. A 0.5 mL aliquot of stock solution (1 mM) of the 1,4-dithiin and 2 mL of solution (35–75 mM) of anthracene were mixed in a 1-cm quartz cell, which was thermostated in a water bath at the specified temperature. The concentration of anthracene was in large excess over that of the 1,4-dithiin, and the rates were measured by following the disappearance of the CT band at 489 nm. The pseudo-first-order rate constants (k_{obs}) were extracted from the slopes of the linear plots of $\ln[(A_t - A_{\infty})/(A_0 - A_{\infty})]$ versus time by a least-squares method (where A_t is the absorbance at time t and A_{∞} is the absorbance after 10 half-lives). The first-order rate constant (k_1) and the equilibrium constant (K) were then obtained from a plot of $[k_{\text{obs}}]^{-1}$ versus the reciprocal anthracene concentration (see Scheme 3).

Acknowledgment. We thank the National Science Foundation and the Robert A Welch Foundation for financial support. We also thank Professor L. Kevan for the use of his X-ray powder diffractometer and S. V. Rosokha for assistance with the solid-state kinetics computations in Scheme 2.

Supporting Information Available: Experimental details of the Mulliken correlation and the Jobs plot for anthracene and the dithiin charge-transfer complex in Figures 11s and 12s, respectively; crystallographic tables for the various CT structures at different degrees of topochemical conversion and for the Diels–Alder adduct (PDF). This material is available free of charge via the Internet at <http://pubs.acs.org>.

JA010108U

(41) Sheldrick, G. M. *SHELXS-86: Program for Crystal Structure Solution*; University of Göttingen: Germany, 1986.

(42) Sheldrick, G. M. *SHELXL93: Program for Refinement of Crystal Structures*; University of Göttingen: Germany, 1993.